

Target Journal

American Journal of Human Genetics

Other ideas: *PLoS Genetics, Genetic Epidemiology*

Title

Adjusting for principal components can induce spurious associations in genome-wide association studies in admixed populations

Authors and Affiliations

Kelsey E. Grinde,^{1*} Timothy A. Thornton,^{2,3} Brian L. Browning,⁴ Sharon R. Browning²

1. Department of Mathematics, Statistics, and Computer Science, Macalester College, Saint Paul, MN, 55105, USA
2. Department of Biostatistics, University of Washington, Seattle, WA, 98195, USA
3. [... Regeneron ...]
4. Division of Medical Genetics, Department of Medicine, University of Washington, Seattle, WA, 98195, USA

* kgrinde@macalester.edu

If we use WHI data, do we need to add Alex as well?

Abstract

Principal component analysis (PCA) is widely used to control for population structure in genome-wide association studies (GWAS). It has been shown that the top principal components (PCs) typically reflect population structure, but deciding exactly how many PCs to include in GWAS regression models can be challenging. Often researchers will err on the side of including more PCs than may be actually necessary in order to ensure that population structure is fully captured. However, through both theoretical results and application to Women's Health Initiative SNP Health Association Resource genotype data and Trans-Omics for Precision Medicine whole genome sequence data for unrelated African American individuals from the Jackson Heart Study (JHS) and Chronic Obstructive Pulmonary Disease Genetic Epidemiology Study (COPDGene), we show that adjusting for extraneous PCs can actually induce spurious associations. In particular, spurious associations arise when PCs capture multiple local genomic features, such as regions of the genome with atypical linkage disequilibrium (LD) patterns, rather than genome-wide ancestry. We show that careful LD pruning prior to running PCA, using stricter thresholds than is often suggested in the literature, can resolve these issues, whereas excluding lists of high LD regions identified in previous studies does not. We also show that the rate of spurious associations can be appropriately controlled when we simply adjust for either the first PC or a model-based estimate of admixture proportions. Our work demonstrates that great care must be taken when using principal components to control for population structure in genome-wide association studies in admixed populations.

1 Introduction

Considerable variability in global ancestry—the genome-wide proportion of genetic material inherited from each ancestral population—has been observed in many studies of admixed populations such as African Americans and Hispanics/Latinos^{1,2,3,4,5}. It has been widely documented that heterogeneous global ancestry, as with other types of population structure, can lead to spurious associations in genome-wide association studies^{6,7,8,9}. In fact, some authors have even cited the ancestral heterogeneity of admixed populations, and the statistical challenges it poses, as one (among many) reason why these populations have been historically underrepresented in genome-wide association studies (GWAS)^{10,11,12,13,14}. Spurious associations can arise in GWAS in ancestrally heterogeneous populations when global ancestry confounds the association between genotypes and the phenotype of interest (Figure 1). This confounding occurs when the genetic variant being tested differs in frequency across ancestral populations (i.e., global ancestry is associated with genotype) and global ancestry also has an effect on the phenotype via, for example, environmental factors or causal loci elsewhere in the genome that differ in frequency across ancestral groups.



Figure 1: Global ancestry (π) confounds the association between the genotype at position j (g_j) and the phenotype of interest (y) if ancestry is associated with both the genotype (e.g., the allele frequencies differ across the ancestral populations) and the phenotype (e.g., there are environmental or other factors that affect the phenotype and differ across the ancestral populations).

A number of methods for detecting and controlling for ancestral heterogeneity in ge-

netic association studies have been proposed. Early approaches included restricting analyses to subsets of ancestrally homogeneous individuals¹⁵, performing a genome-wide correction for test statistic inflation due to ancestral heterogeneity via *genomic control*⁶, and using family-based designs¹⁶. More recently, approaches based on mixed models have been proposed^{17,18,19}, using random effects to control for both close (e.g., due to family-based sampling) and distant (e.g., due to shared ancestry) relatedness across individuals. When studies do not include closely related individuals, a simpler approach is to include inferred global ancestry as a fixed effect in marginal regression models^{7,20}. This fixed effects adjustment for global ancestry is used extensively throughout the literature, with global ancestry inferred using either model-based ancestry inference methods (e.g., `frappe`²¹, `STRUCTURE`²², `ADMIXTURE`²³, `RFMix`²⁴) or principal component analysis (e.g., `EIGENSTRAT`⁷, `SNPRelate`²⁵, `PC-AiR`²⁶).

Principal component analysis (PCA) is a widely-implemented unsupervised approach for inferring global ancestry that offers the advantages of not requiring reference panel data or pre-specification of the number of ancestral populations of interest. It is also capable of capturing sub-continental structure²⁷. To infer global ancestry using PCA, we perform a singular value decomposition of the matrix of standardized genotypes (i.e., $\mathbf{X} = \mathbf{UDV}^\top$) or, equivalently, an eigenvalue decomposition of the genetic relationship matrix (i.e., $\mathbf{XX}^\top = \mathbf{UD}^2\mathbf{U}^\top$). It has been shown that top eigenvectors, or *principal components* (PCs), $\mathbf{u}_1, \mathbf{u}_2, \dots$ tend to reflect global ancestry^{28,29}. To adjust for ancestral heterogeneity in genome-wide association studies, we choose some number of PCs to include as covariates in our GWAS regression models.

Determining the number of PCs needed to capture global ancestry is non-trivial. Numerous techniques have been proposed, including formal significance tests based on Tracy-Widom theory^{28,7}, examining inflation factors^{30,5} and/or the proportion of variance explained by each PC^{31,30,5}, comparing PCs to self-reported race/ethnicity⁵, and keeping PCs that are significantly associated with the trait^{32,33}. Typically, the number of PCs selected is on the order

of one to ten³⁴, but in practice it is not uncommon to see applications in which more many more PCs are used—more even than may actually be necessary to capture global ancestry. This could be due in part to work that has suggested that including higher-order PCs can provide the safeguard of removing “virtually all stratification”³⁵ at the cost of perhaps only “subtle” decreases in power³⁶.

Another challenge that can arise in using PCA to adjust for ancestral heterogeneity involves ensuring that PCs actually reflect global ancestry and not some other features or artifacts of the data. Prior work has shown that PCs can capture relatedness across samples^{28,9,37,26}, array artifacts or other data quality issues^{28,7,9,38}, and/or small regions of the genome with unusual patterns of linkage disequilibrium (LD)^{28,7,39,40,41,9,38,42,43,37,44}. To address this last issue, many authors have suggested running PCA on a reduced subset of variants after first performing *LD pruning*, using a program such as PLINK⁴⁵ to remove variants that are in “high” LD (e.g., pairwise-correlation $r^2 > 0.2$) with nearby variants^{39,46,27,47,48,49,38,43,37,50,26,30,51,5,33}, and/or excluding regions of the genome that are known to have extensive, long-ranging, or otherwise unusual patterns of LD^{39,46,27,41,49,38,31,5}. A list of these previously-identified high LD regions and references that recommend their exclusion are provided in Table 1.

The above-cited suggestions regarding LD pruning and filtering are not universally implemented and the downstream implications of adjusting for PCs that capture features other than global ancestry are not fully understood. Furthermore, much of this prior work was conducted in populations of European ancestry, so recommendations on how best to implement principal component-based adjustment for ancestral heterogeneity in admixed populations are lacking. In this paper, we investigate the impact of LD filtering and pruning choices, as well as choices of the number of principal components to include in analyses, on genome-wide association studies in admixed populations. We show that principal components may capture local genomic features, unless careful pre-processing is performed prior to analysis. We also conduct simulation studies and provide analytic results to show that including too many PCs

Chr	Start (bp)	End (bp)	References
1	48000000	52060567	49,41,38
2	85941853	100500000	49,41,38
2	129600000	140000000	41,27,38,31,5,52
2	182882739	190000000	49,41,38
3	47500000	50000000	49,41,38
3	83500000	87000000	49,41,38
3	89000000	97500000	41,38
3	163100000	164900000	52
5	44000000	51500000	46,49,41,38
5	98000000	100500000	41,38
5	129000000	132000000	49,41,38
5	135500000	138500000	41,38
6	23800000	39000000	46,49,41,27,38,31,5,52
6	57000000	64000000	49,41,38
6	140000000	142500000	49,41,38
7	55000000	66193285	49,41,38
8	6300000	13500000	46,49,41,27,40,38,31,5,52
8	43000000	50000000	49,41,38
8	112000000	115000000	49,41,38
10	37000000	43000000	49,41,38
11	45000000	57000000	46,41,38
11	87500000	90500000	49,41,38
12	33000000	40000000	49,41,38
12	109500000	112021663	41,38
14	46600000	47500000	52
17	37800000	42000000	27,5
20	32000000	34500000	49,41,38

Table 1: Regions of the genome with high, long-range, or otherwise unusual patterns of linkage disequilibrium (LD) that are often recommended for exclusion prior to running PCA. This list of regions was generated on the basis of an extensive literature review. Start and end physical (base pair) positions are provided with respect to genome build 36. Also available for download (in builds 36, 37, or 38) at <https://github.com/kegrinde/PCA/>.

can actually induce spurious associations in GWAS, particularly when those extraneous PCs capture local genomic features rather than genome-wide ancestry. To conclude, we provide suggestions regarding best practice for appropriately controlling for ancestral heterogeneity in genome-wide association studies in admixed populations.

2 Material and Methods

2.1 Data and Quality Control

Our analyses focus on genotype and sequence data from three samples of unrelated African American individuals. In particular, we consider genotype data from the Women’s Health Initiative SNP Health Association Resource (WHI SHARe), as well as whole genome sequencing data from two contributing studies to the Trans-Omics for Precision Medicine (TOPMed) Whole Genome Sequencing Project: the Jackson Heart Study (JHS) and the Genetic Epidemiology of Chronic Obstructive Pulmonary Disease Study (COPDGene). We performed quality control (QC) and identified subsets of unrelated African American individuals prior to running any further analyses.

2.1.1 WHI SHARe Genotype Data

The Women’s Health Initiative (WHI) is a long-term study of the health of women in the United States. In total, 161,808 postmenopausal women aged 50–79 years old were recruited to participate in this study. Additional details on study design and cohort characteristics can be found elsewhere⁵³. Included in the WHI study are 12,151 self-identified African American women who consented to genetic research, a subsample of which were selected for genotyping using the Affymetrix Genome-Wide Human SNP Array 6.0. This array contains 906,000 single nucleotide polymorphisms (SNPs) and more than 946,000 probes for the detection of copy number variants; in these analyses, we focus only on the SNPs.

The genotype data were processed for quality control, including call rate, concordance

rates for blinded and unblinded duplicates, and sex discrepancy, leaving 871,309 unflagged SNPs with a genotyping rate of 99.8% and 8,421 African American women³². We additionally used the iterative procedure suggested by Conomos et al.⁵⁴ to identify a subset of 8,064 mutually unrelated individuals, using a kinship threshold of 0.044 (i.e., excluding first, second, and third degree relatives).

2.1.2 TOPMed Whole Genome Sequence Data

The Trans-Omics for Precision Medicine (TOPMed) Whole Genome Sequencing Project is an ongoing project sponsored by the National Heart, Lung, and Blood Institute (NHLBI). The goal of this project is to collect and analyze whole-genome sequences, other omics data, and rich phenotypic information for over 100,000 individuals from diverse backgrounds. Data are periodically released on dbGaP for analysis by the broader scientific community. Our analysis uses data from *freeze 4*, released in 2017, and *freeze 5b*, released in 2018. These two freezes include samples from a large number of contributing studies. We focus on two such studies: the Jackson Heart Study (JHS) (accession number: phs000964) and the Genetic Epidemiology of Chronic Obstructive Pulmonary Disease Study (COPDGene) (accession number: phs000951). In total, the freeze 4 JHS dataset includes 3,406 African American individuals and the freeze 5b COPDGene dataset includes 8,742 African American and European American individuals. For TOPMed freezes 4 and 5b, high coverage ($\approx 30X$) whole genome sequencing was performed by several sequencing centers. Variant discovery and genotype calling was performed by the TOPMed Informatics Resources Center (IRC) using the GotCloud pipeline⁵⁵.

Quality control (QC) was performed by the sequencing centers, IRC, and TOPMed Data Coordinating Center, and only those samples and variants that passed these stages of QC are included in the Variant Call Format (VCF) files downloaded from dbGaP. Details on TOPMed sequencing and QC methods are available in Taliun et al.⁵⁶ and on the TOPMed website: <https://topmed.nhlbi.nih.gov/data-sets>. Prior to genetic ancestry inference, we

performed two additional stages of variant- and sample-level filtering. We used `bcftools`⁵⁷ to remove indels and otherwise restrict our analyses to biallelic single nucleotide variants (SNVs). Finally, we used the University of Washington Genetic Analysis Center TOPMed analysis pipeline to restrict our analyses to a subset of mutually unrelated individuals (kinship threshold = 0.044)⁵⁴. After filtering, 2,777 and 8,476 samples and 77,136,850 and 135,522,041 variants remained in JHS and COPDGene, respectively.

2.2 Genetic Ancestry Inference

We consider two approaches to inferring genetic ancestry in these admixed samples: model-based approaches and principal component analysis.

2.2.1 Model-Based Approaches

In WHI SHARe African Americans, we inferred both local and global genetic ancestry using model-based ancestry inference techniques. Local ancestry inference was performed using **RFMix**²⁴ and a reference panel including individuals of European and African decent from the International HapMap Project (HapMap)⁵⁸: see Grinde et al.⁵⁹ for more details. We then calculated global ancestry proportions via the genome-wide average local ancestry $\hat{\pi}_{ik} = \frac{1}{2m} \sum_{j=1}^m a_{ijk}$, where a_{ijk} is the inferred number of alleles (0, 1, or 2) inherited by individual i at variant j from ancestral population k . We also compared these **RFMix**-based global ancestry estimates to results from supervised and unsupervised **ADMIXTURE**²³ analyses with two ancestral populations ($K = 2$). The supervised analysis used the same HapMap reference panel as was used to infer local ancestry using **RFMix**. All three sets of admixture proportions were highly correlated (pairwise Pearson correlation > 0.998), so we focus on the **RFMix**-based admixture proportion estimates for the remainder of our analyses.

In TOPMed JHS and COPDGene samples, we inferred global ancestry via unsupervised **ADMIXTURE** analyses with both two and three ancestral populations (i.e., $K = 2$ and $K = 3$). We also used these inferred global ancestry proportions to identify subsets of admixed indi-

viduals. In particular, the COPDGene study includes both African American and European American individuals, but self-identified race/ethnicity information was not available from dbGaP. Instead, we used inferred admixture proportions to identify and restrict our attention to individuals with at least 29.5% African ancestry. The choice of threshold follows from the results reported by Parker et al.⁶⁰, showing that the self-identified African American individuals in the COPDGene study have inferred proportions of African ancestry ranging from 29.5% and above. (Note that we are not suggesting that this same threshold be universally applied to identify African American individuals in other samples.) After filtering, 2,676 individuals remain. In addition, although JHS is known to focus on African Americans, we did identify some individuals inferred to have 100% European ancestry in that sample. These individuals were excluded from further analyses, leaving a total of 1,888 admixed samples.

2.2.2 Principal Component Analysis

We ran PCA on the WHI SHARe genotype data using **SNPRelate**²⁵. First, we applied PCA to the set of all 551,025 SNPs with available genotypes. We refer to these PCs as the *naively generated PCs*. We also applied PCA to subsets of SNPs based on the following pre-processing criteria: excluding SNPs falling into regions of the genome that have been cited in the literature as potentially problematic for PCA (Table 1), LD pruning with an r^2 threshold of 0.1 and window size of 0.5 mega basepairs (Mb), or both literature-based exclusions and LD pruning. LD pruning and literature-based filters were implemented using the **SNPRelate** package. Table 2 summarizes the number of SNPs remaining after each set of pre-processing steps. After running PCA on these different sets of variants, we also used **SNPRelate** to assess the contribution of each SNP to each principal component by calculating the correlation between PCs and genotypes, as well as the SNP loadings.

In TOPMed JHS and COPDGene samples, we used the University of Washington Genetic Analysis Center (UW GAC) pipeline to implement pre-processing, run principal component analysis, and calculate and visualize the contribution of individual variants to each PC.

	WHI SHARe	TOPMed JHS	TOPMed COPDGene
Neither Exclude nor Prune	551,025	14,117,957	13,959,378
Exclude High LD Regions (Table 1)	536,668	13,723,944	13,575,038
LD Prune ($r^2 < 0.1$, 0.5 Mb windows)	49,723	245,003	251,040
Both Exclude and Prune	48,794	239,425	245,378

Table 2: Number of autosomal variants remaining after different combinations of pre-processing steps were applied prior to running PCA. Note that TOPMed analyses additionally applied a filter to keep only those variants with minor allele frequency greater than 0.01.

Similar to WHI SHARe, we applied PCA to various subsets of variants based on different pre-processing criteria, including a *naive* analysis with no prior LD-based pruning or filtering, an analysis after *excluding* the regions listed in Table 1, an analysis after LD *pruning* with an r^2 threshold of 0.1, and an analysis after both LD-based pruning and filtering. Following the recommendations of Kirk⁶¹ and the UW GAC pipeline documentation, we also removed variants with a minor allele frequency lower than 0.01 in all cases. Note that the UW GAC pipeline does provide the option to exclude some of the regions listed in Table 1 (the *LCT* gene on chromosome 2, the HLA region on chromosome 6, and the locations of large inversions on chromosomes 8 and 17), but we customized the pipeline code slightly to add the other regions identified in our literature review. See Table 2 for the number of variants included in each analysis.

2.3 Simulation Study

To explore the impact of adjusting for principal components that capture local genomic features, we conducted a simulation study using genotype data and simulated traits in the WHI SHARe African American sample.

2.3.1 Trait Simulation

Traits were simulated for each individual $i = 1, \dots, 8064$ such that they depended only on the genotype g_{ij} at a single causal variant with effect size β_j :

$$y_i = \beta_j g_{ij} + \epsilon_i, \quad \epsilon_i \stackrel{iid}{\sim} N(0, 1).$$

We considered seven choices of effect sizes ($\beta_j = 0, 0.25, 0.5, 1, 2, 4, 8$) and 473 choices for the position j of the causal variant, varying the position of this causal variant across all 22 autosomes.

To choose the location of these causal variants, we first estimated the difference in ancestral allele frequencies for each variant using the observed allele frequencies in our HapMap reference panel (which included samples from the CEU (Utah residents with Northern and Western European ancestry) and YRI (Yoruba in Ibadan, Nigeria) populations: see Grinde et al.⁵⁹ for more details). We also considered the SNP loadings for the set of PCs that were generated without any prior LD-based filtering or pruning. We identified the 10 variants on each chromosome with the highest absolute SNP loading for each of the first four PCs. In total, 373 unique variants were selected according to this procedure. For comparison, we also selected 100 variants across the autosomes with low SNP loadings ($|\text{loading}| < 0.0008$) for all of the first four PCs. Among these 100 variants, 85 were selected such that they had different allele frequencies in the African and European ancestral populations ($|\hat{p}_{CEU} - \hat{p}_{YRI}| > 0.6$), and 15 were selected that had similar allele frequencies in the two ancestral populations ($|\hat{p}_{CEU} - \hat{p}_{YRI}| < 0.005$).

2.3.2 GWAS Models

For each simulated trait, we ran genome-wide association studies using models of the general form

$$E[y_i | g_{ij}, \mathbf{w}_i] = \alpha + \beta_j g_{ij} + \boldsymbol{\gamma} \mathbf{w}_i,$$

where y_i is the simulated quantitative trait, g_{ij} is the genotype at position j , and \mathbf{w}_i is a vector of additional covariates. Note that we quantify genotype g_{ij} by the number of copies—0, 1, or, 2—of some pre-specified allele (e.g., the minor allele) carried by individual i at position j . We fit these models at every position $j = 1, \dots, m$ across the genome and test for association between the trait and genotype by testing the null hypothesis $H_0 : \beta_j = 0$ using a traditional Wald test.

In particular, we consider four models: a model making no adjustment for ancestral heterogeneity (i.e., $\mathbf{w}_i = \emptyset$), a model adjusting for model-based admixture proportions ($\mathbf{w}_i = \hat{\pi}_i$), a model adjusting for the first principal component ($\mathbf{w}_i = u_{1i}$), and a model adjusting for the first four principal components ($\mathbf{w}_i = [u_{1i} \ u_{2i} \ u_{3i} \ u_{4i}]$). For the models adjusting for principal components, we consider four sets of PCs based on different pre-processing criteria: *none* (no prior LD-based exclusions or pruning), *exclusions only* (excluding regions from Table 1 but no LD pruning), *pruning only* (LD pruning with $r^2 < 0.1$ and a window size of 0.5 Mb, but not excluding regions from Table 1), and *both* (both Table 1 exclusions and LD pruning).

2.3.3 Spurious Associations

To evaluate these ancestral heterogeneity adjustment approaches, we compared the number of spurious associations that appeared when we used each model. We quantified spurious associations by counting the number of chromosomes, not including the chromosome on which the causal variant was located, with at least one variant reaching genome-wide significance. For all models, the genome-wide significance threshold was set to the $p = 5.0 \times 10^{-8}$ threshold that is used extensively throughout the GWAS literature^{62,63}.

2.4 Data and Software Availability

WHI SHARe genotype data and TOPMed whole genome sequence data are available for analysis upon request and application. Visit study sites and dbGaP for more information.

All software packages used throughout this paper are freely available online:

- bcftools⁵⁷ (quality control): <https://samtools.github.io/bcftools/>
- RFMix²⁴ (local ancestry inference): <https://sites.google.com/site/rfmixlocalancestryinference/>
- ADMIXTURE²³ (global ancestry inference): <https://dalexander.github.io/admixture/>
- PCRelate⁵⁴ and PC-AiR²⁶ (identifying unrelated individuals): <https://rdrr.io/bioc/GENESIS/>
- SNPRelate²⁵ (LD pruning, PCA, and PCA-related diagnostics):
<https://www.bioconductor.org/packages/release/bioc/html/SNPRelate.html>
- PLINK⁴⁵ (GWAS): <https://zzz.bwh.harvard.edu/plink/>
- TOPMed Analysis Pipeline (identifying unrelated individuals, LD pruning, PCA, PCA-related diagnostics, and association studies in whole genome sequence data):
https://github.com/UW-GAC/analysis_pipeline
- R (analyzing and visualizing results): <https://cran.r-project.org/>

Other resources pertaining to this paper, including download-able lists of the high LD regions in Table 1 in various builds, can be found on the lead author’s GitHub page: <https://github.com/kegrinde/PCA>.

3 Results

3.1 Ancestral heterogeneity in admixed populations

Inferred admixture proportions for three samples of African American individuals are presented in Figure 2.

In WHI SHARe African Americans, we compared admixture proportion estimates from a variety of model-based techniques. Figure 2 presents admixture proportions estimated

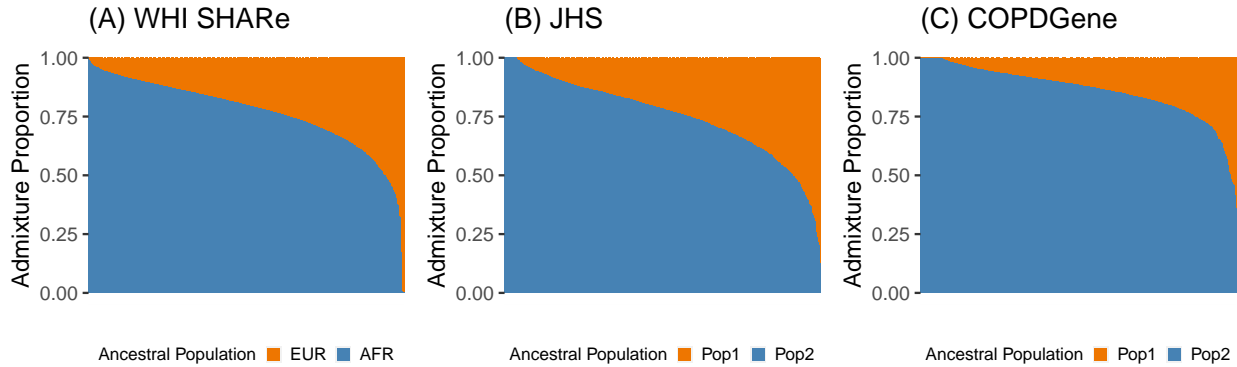


Figure 2: Barplots of estimated admixture proportions in (A) WHI SHARe, (B) TOPMed JHS, and (C) TOPMed COPDGene African Americans.

as genome-wide average local ancestry, using local ancestry calls from `RFMix`. These local ancestry based admixture proportion estimates were highly correlated (Pearson correlation > 0.998) with admixture proportions from supervised and unsupervised `ADMIXTURE` analyses with two ancestral populations ($K = 2$).

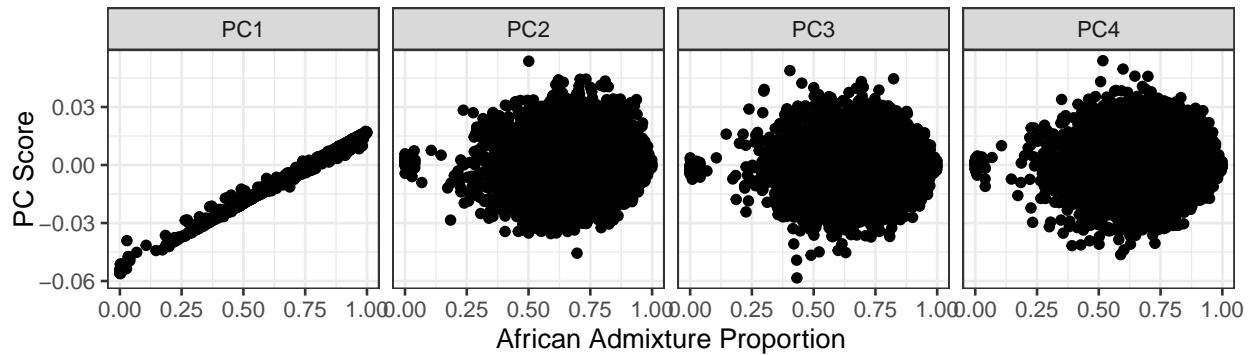
In TOPMed samples, we performed unsupervised `ADMIXTURE` analyses with varying numbers of ancestral populations. Figure 2 presents results with $K = 2$. Although these analyses were unsupervised, based on prior studies of admixture in African Americans, and in comparison to the distribution of admixture proportions seen here in WHI SHARe, we believe that the ancestral population colored orange (Pop1) in Figure 2 corresponds to European ancestry and the population colored in blue (Pop2) corresponds to African ancestry.

In all three samples, we observe considerable variability in the relative proportions of African and European ancestry across individuals. This ancestral heterogeneity motivates the need to carefully adjust for global ancestry in genome-wide association studies in these, just as in other, admixed samples.

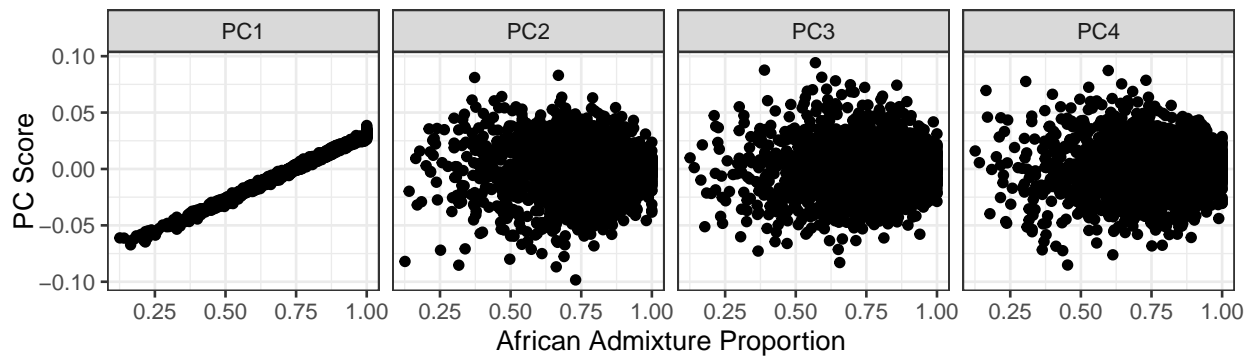
3.2 First PC captures global ancestry

In an African American population, we might expect that only one principal component is needed to capture ancestral heterogeneity, at least with respect to differences in the relative

(A) WHI SHARe



(B) JHS



(C) COPDGene

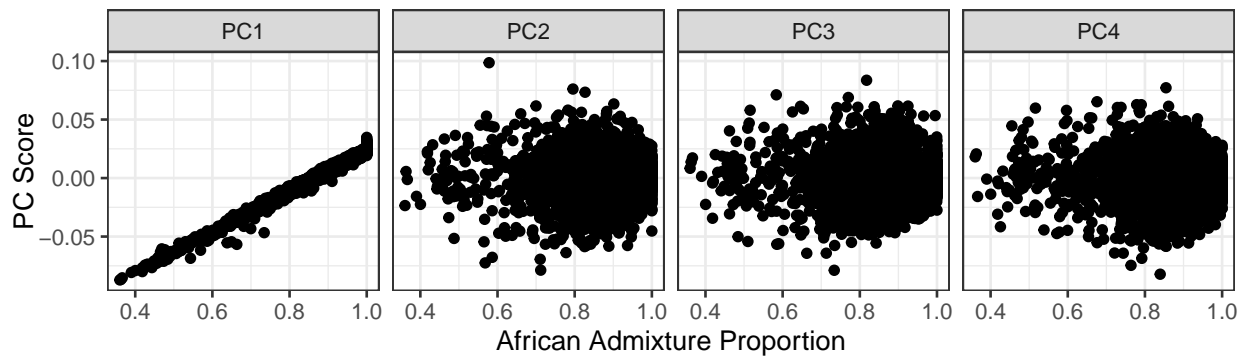


Figure 3: Scatterplots of estimated African admixture proportions versus the first four PCs in (A) WHI SHARe, (B) TOPMed JHS, and (C) TOPMed COPDGene African Americans. Here we consider PCs that were generated without any prior LD-based filtering or pruning.

proportion of African and European continental ancestry. Comparing model-based admixture proportions to principal components in WHI SHARe, JHS, and COPDGene confirms this hypothesis. In all three samples of African Americans, the first principal component is highly correlated with the inferred proportion of African ancestry, while later PCs show very little correlation with genome-wide continental ancestry (Figure 3). We observe similar patterns of correlation between PCs and inferred admixture proportions regardless of the type of LD filtering (or lack therof) performed prior to running PCA (Supplemental Figure 9).

3.3 Later PCs may capture local genomic features

As we see in Figure 3, in African American samples the first principal component seems to be capturing global ancestry, whereas later PCs are not. While it is possible that these higher-order principal components may be capturing sub-continental structure that is not captured by the model-based admixture proportions, we see in many cases that these later PCs are actually capturing local genomic features rather than genome-wide ancestry. This is evident upon inspection of *SNP loadings*, which represent the contribution of each variant to each principal component, or in investigating the correlation between principal component scores and the original genotypes.

Figure 4 presents the correlation between principal components and genotypes in JHS and COPDGene African Americans when PCs are generated without any prior LD-based pruning or filtering. We see that variants across the genome are contributing relatively equally to the first principal component, whereas the second, third, and fourth PCs are driven more-so by variants on a select number of chromosomes. In JHS, for example, the second PC is particularly highly correlated with variants on chromosomes 6 and 8, and less so with variants on 2, 3, and 11. We see similar patterns, although with peaks on different combinations of chromosomes, in COPDGene (Figure 4B) and WHI SHARe African Americans (leftmost column of Figure 5). The peaks in these genotype-PC correlation plots indicate that those

principal components are primarily capturing variation at a handful of positions along the genome rather than genome-wide global ancestry.

Note that these patterns differ slightly from what has previously been observed in European populations. In particular, in European populations a principal component might capture variation on a single chromosome (e.g., see Supplemental Figure 13), whereas here in these admixed populations we see PCs driven by contributions from variants across several chromosomes.

3.4 Impact of LD pruning

Previous authors have suggested that this phenomenon of principal components capturing local genomic features arises due to high or otherwise unusual patterns of linkage disequilibrium among variants; as a result, they recommend that variants in high LD with one another be removed prior to running PCA. Following these recommendations, we compare the set of principal components based on all variants to PCs generated after first removing regions of the genome known to have high LD (Table 1), performing LD pruning, or both.

Figure 5 illustrates the impact of these pre-processing steps on the correlation between genotypes and PCs in WHI SHARe African Americans. Recall that the leftmost column of Figure 5 presents results for principal components that were generated without any prior LD-based filtering or pruning, and we see that PCs 2–4 are capturing local genomic features on a select number of chromosomes rather than genome-wide ancestry. When we exclude the previously-identified high LD regions reported in Table 1 before running PCA (the second column of Figure 5), the pattern of *which* SNPs are driving PCs 2–4 changes, but the issue of PCs capturing local genomic features has not been resolved. However, after LD pruning with an r^2 threshold of 0.1 and a window size of 0.5 Mb (third column), we now see similar patterns with PCs 2–4 as we do with the first principal component — all variants are now contributing relatively equally to each PC. If we then also remove previously-identified high LD regions in addition to performing LD pruning (rightmost column), the patterns of

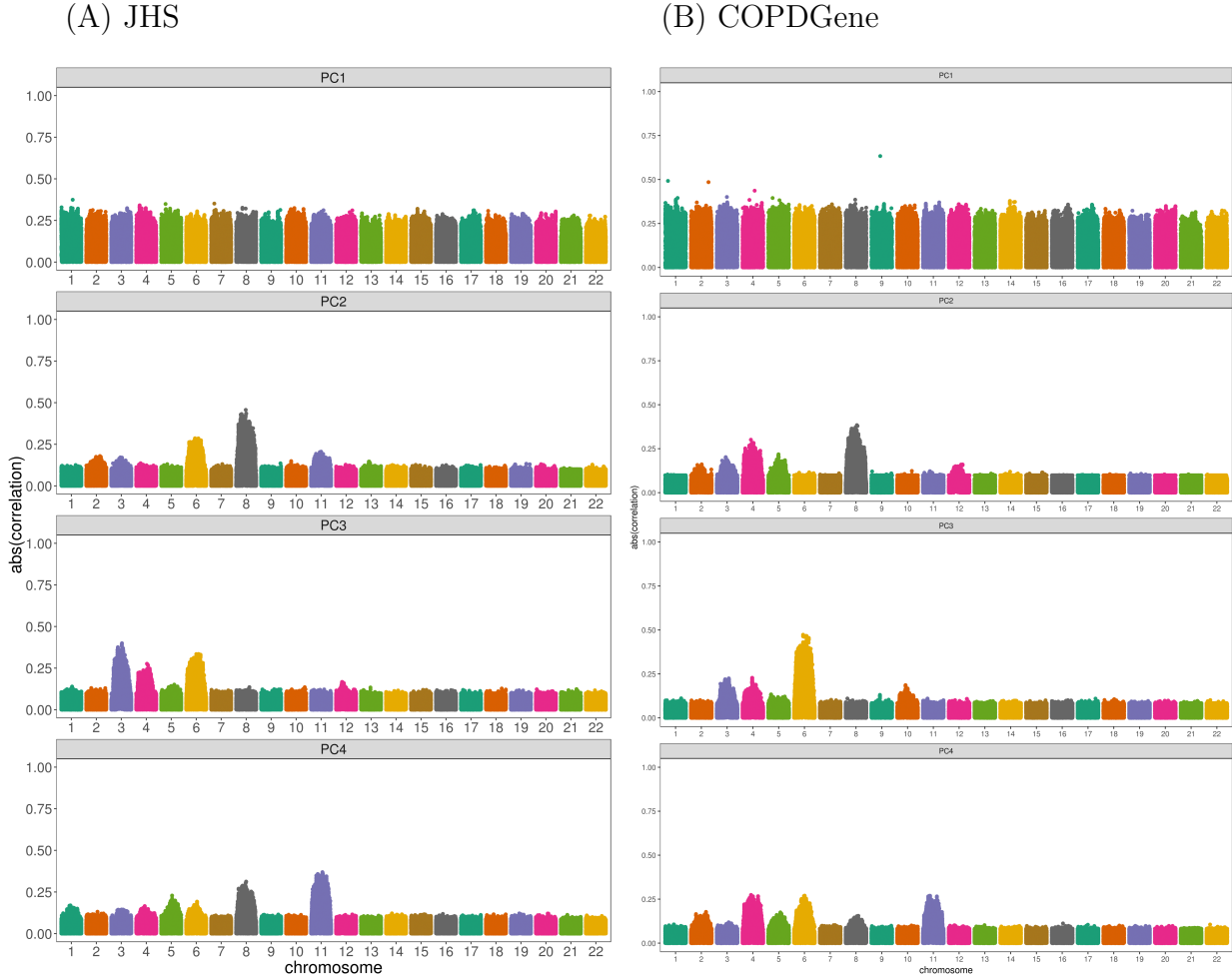


Figure 4: Correlation between naively generated PCs (i.e., PCs that were constructed without any prior LD-based filtering or exclusions) and genotypes in JHS and COPDGene African Americans. Each panel plots the absolute value of the correlation between principal components and genotypes (on the y-axis) versus the position along the genome (x-axis). Panels are organized vertically according to which PC is being investigated (1, 2, 3, 4) and horizontally according to the sample (A: JHS, B: COPDGene). Peaks in this plot indicate that a variant has a larger *loading*, i.e., a larger contribution to that principal component.

correlation between PCs and genotypes are indistinguishable from those with LD pruning alone.

Note that the thresholds for LD pruning that we use here ($r^2 < 0.1$) are stricter than the default for many software programs and the threshold used in many studies of European populations ($r^2 < 0.2$). If we use this default r^2 threshold, we see improvement for the second and third principal components, but the fourth continues to capture local genomic features on a small number of chromosomes (Supplemental Figure 10). Similar patterns are observed in JHS and COPDGene.

3.5 Adjusting for PCs that capture local genomic features can induce spurious associations

We have demonstrated that, especially without strict LD pruning, principal components can capture local genomic features rather than global ancestry in admixed populations. However, it remains to be fully understood what the downstream implications would be of adjusting for these PCs in genome-wide association studies. We conducted a simulation study to investigate these implications further.

Figure 6 presents Manhattan plots from one replicate of our simulation study. In this setting, there is a single causal variant on chromosome 4, and we compare the results from genome-wide association studies in WHI SHARe African Americans using different ancestral heterogeneity adjustment approaches. As expected, we see extreme inflation, i.e., statistically significant associations on *every* chromosome, when we do not make any adjustment for ancestral heterogeneity (Panel A). Otherwise, when we infer and adjust for ancestral heterogeneity using either PCA or a model-based approach, we see a single peak in our Manhattan plot on chromosome 4—as hoped, given that is where the causal variant is located—with one notable exception. When we adjust for the first four principal components (as has been done in previous GWAS in WHI SHARe^{32,64}), where those PCs were generated without any prior LD-based pruning or filtering, then we see a spurious association on chromosome 6

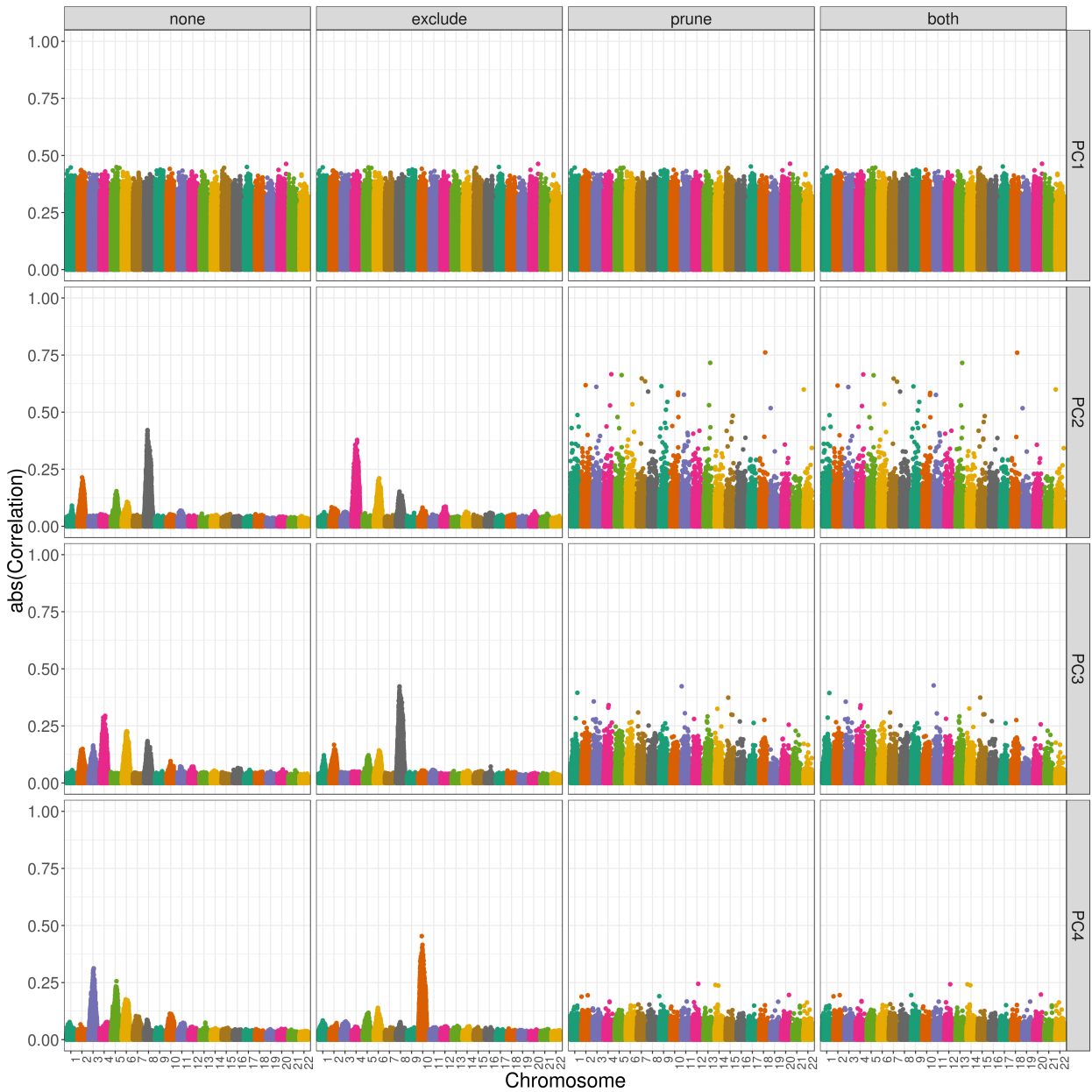


Figure 5: Correlation between PCs and genotypes in WHI SHARe African Americans with different choices of pre-processing. Each panel plots the absolute value of the correlation between principal components and genotypes (on the y-axis) versus the position along the genome (x-axis). Panels are organized vertically according to which PC is being investigated (1, 2, 3, 4) and horizontally according to the level of filtering that was applied prior to running PCA (*none*: all SNPs, *exclude*: after excluding regions in Table 1, *prune*: after LD pruning with an r^2 threshold of 0.1 and window size of 0.5 Mb, and *both*: after both exclusions and LD pruning).

(Panel C). However, this spurious association disappears if we only adjust for the first of these PCs (Panel B). Likewise, no spurious association arises if we adjust for model-based admixture proportions (Panel D) or if we use PCs that were generated after LD pruning and Table 1 exclusions (Panels E and F). Note that the causal variant, on chromosome 4, and the spurious signal, on chromosome 6, are both located in regions of the genome that are highly correlated with the PCs that were generated without any prior LD pruning (Figure 5).

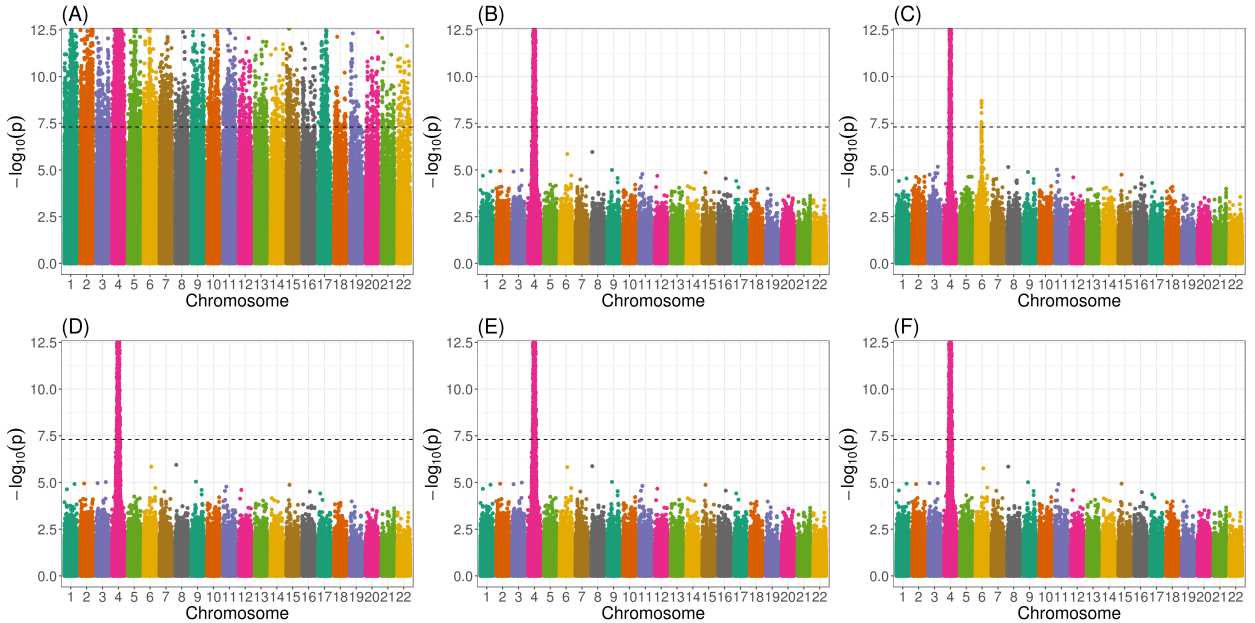


Figure 6: Manhattan plots from genome-wide association studies in WHI SHARe African Americans using different approaches to adjust for ancestral heterogeneity. In this example, the simulated trait depends only on the genotype at a single variant on chromosome 4: $y \sim N(g_{rs2036153}, 1)$. Panels present results using different adjustment approaches: (A) no adjustment; (B) one PC, with PCs calculated using all variants; (C) four PCs, with PCs calculated using all variants; (D) model-based admixture proportion estimates; (E) one PC, with PCs calculated after LD pruning ($r^2 < 0.1$, window size = 0.5 Mb) and Table 1 exclusions; and (F) four PCs, with PCs calculated after LD pruning and exclusions.

These results are not unique to this simulation setting. Figure 7 presents a comparison of the rate of spurious associations in genome-wide association studies in WHI SHARe African Americans. We see that, across all simulation settings (Panel A), adjusting for PCs that capture local genomic features leads to higher numbers of spurious associations, on

average. Comparing models that make some sort of adjustment for ancestral heterogeneity, we observe the most spurious associations when GWAS models adjust for four principal components that were generated without any LD-based pruning or exclusions. Excluding the high LD regions from Table 1 prior to running PCA reduces the number of observed spurious associations slightly, but not to the levels of the other approaches. Given what we saw in Figure 5, this is not surprising: even with these exclusions, PCs 2–4 still capture local genomic features—unless those exclusions are also combined with strict LD pruning. We see fewer spurious associations when models adjust for model-based admixture proportions or principal components that do not capture local genomic features (i.e., using just the first PC, regardless of LD-based pruning or exclusions, or adjusting for four PCs when LD pruning was performed).

3.6 Factors that influence the rate of spurious associations

Our simulation results highlight various factors that influence when, and how many, spurious associations arise when adjusting for PCs that capture local genomic features. First, we note that there are very few spurious associations, regardless of the adjustment approach (or even lack thereof), when there are small differences in ancestral allele frequencies at the causal variant (Figure 7B). This is to be expected: in this scenario, the causal variant is not associated with global ancestry, so global ancestry is not a confounding variable (Figure 1) and there is no need for adjustment. Considering other simulation settings in which the causal variant has a larger difference in ancestral allele frequencies (panels C, D, and E of Figure 7), so adjusting for ancestral heterogeneity is needed, the number of observed spurious associations remains low for models that adjust for admixture proportions, a single principal component (regardless of pre-processing), or four PCs—if those PCs were generated after strict LD pruning. For the two models that adjust for PCs capturing local genomic features (i.e., the models that adjust for 4 PCs that were generated with or without Table 1 exclusions, but no LD pruning), however, we see a higher rate of spurious associations,

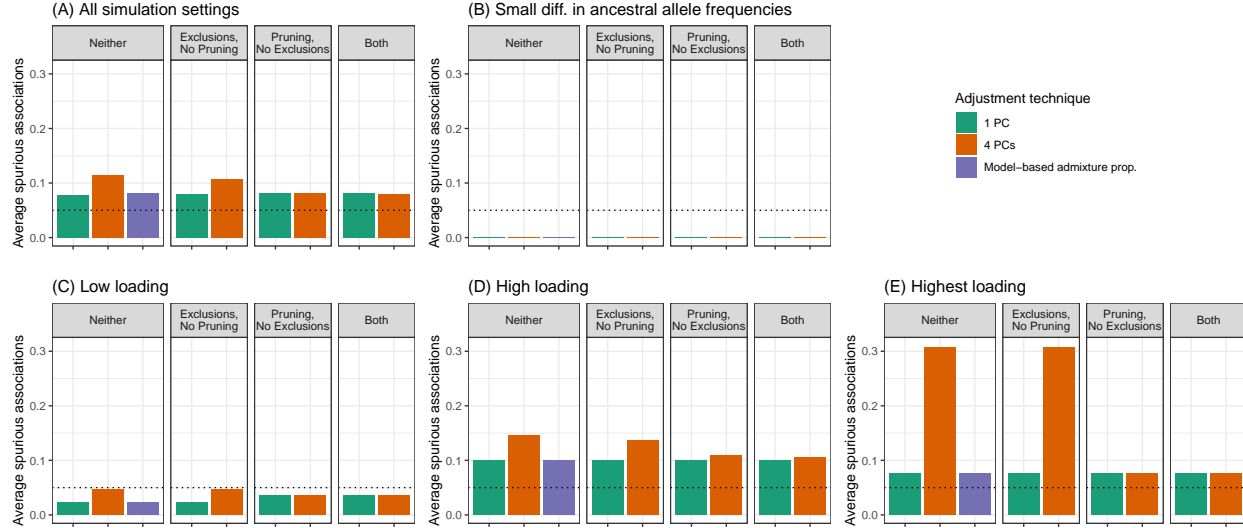


Figure 7: Comparison of the number of spurious associations in genome-wide association studies in WHI SHARe African Americans using different approaches to adjust for ancestral heterogeneity. Panels display the average number of spurious associations that were observed across (A) all simulation settings, or across the subset of simulation settings in which the causal variant has (B) a small difference in ancestral allele frequencies, (C) low SNP loadings for each of the first four PCs, (D) a high SNP loading for at least one of the first four PCs, or (E) the highest SNP loading on its chromosome for one of the first four PCs. Within each panel, we compare the number of spurious associations when GWAS models adjust for model-based admixture proportions, 1 PC (with or without LD pruning and/or Table 1 exclusions), or 4 PCs (with or without LD pruning and/or Table 1 exclusions). Results shown here are for simulated traits with a single causal variant with an effect size (β) of 1. See Supplemental Figure 14 for results with other choices of β .

particularly when the causal variant is highly correlated with one of those PCs. Notably, as the size of the causal variant's SNP loading increases from low (Figure 7C), to high (Figure 7D), to the highest on its chromosome (Figure 7E), we see an increasing number of spurious associations for these two approaches. This confirms the pattern we saw in Figure 6, where a spurious association arose when we adjusted for PCs that were highly correlated with variants in several regions across the genome, and both the causal variant and spurious signal were located in one of those regions. Finally, we note that these problems worsen as the effect size of the causal variant increases (see Supplemental Figure 14).

To better understand the patterns observed in our simulation study, we compare the expected effect size estimates from GWAS models in admixed populations with two ancestral

populations using different techniques for adjusting for ancestral heterogeneity. As in our simulations, we assume that the trait depends on a single causal variant:

$$y_i \stackrel{iid}{\sim} N(\beta_1 g_{i1} + \beta_\pi \pi_i, 1),$$

where g_{i1} represents the number of minor alleles carried by individual i at the causal variant, which we will refer to as *Variant 1*, and π_i is the individual's admixture proportion. (Note that $\beta_\pi = 0$ in our simulation study, but we consider the more general setting here.) We can then derive the expected effect size estimate at that causal variant, as well as a second variant that is not associated with the trait and sits on a different chromosome than the causal variant. When we consider a GWAS model that adjusts for the true admixture proportions, the expected effect size estimates at the causal variant (Variant 1) and the unlinked neutral variant (Variant 2) are

$$E[\hat{\beta}_1] = \beta_1$$

$$E[\hat{\beta}_2] = 0,$$

where β_1 is the true effect size of the causal variant and $\beta_2 = 0$ is the true effect size of the neutral variant. In other words, models that perfectly adjust for ancestral heterogeneity will yield unbiased estimates of the effect size at the causal and unlinked neutral variants.

In comparison, GWAS models that do not make any adjustment for ancestral heterogeneity will yield effect size estimates of

$$\begin{aligned} E[\hat{\beta}_1] &= \beta_1 + \frac{(p_{11} - p_{10})V_\pi\beta_\pi}{p_{10}(1 - p_{10}) + (p_{11} - p_{10})(1 - p_{11} - p_{10})E_\pi + (p_{11} - p_{10})^2(V_\pi + E_\pi - E_\pi^2)} \\ E[\hat{\beta}_2] &= 0 + \frac{(p_{21} - p_{20})V_\pi\{\beta_\pi + 2\beta_1(p_{11} - p_{10})\}}{p_{20}(1 - p_{20}) + (p_{21} - p_{20})(1 - p_{21} - p_{20})E_\pi + (p_{21} - p_{20})^2(V_\pi + E_\pi - E_\pi^2)}, \end{aligned}$$

where E_π, V_π are the population mean and variance of the admixture proportions, β_π is the direct effect of admixture proportions on the trait, p_{11}, p_{10} are the allele frequencies of the causal variant in the two ancestral populations, and p_{21}, p_{20} are the ancestral allele frequencies of the unlinked neutral variant. From these results, we see that the unadjusted

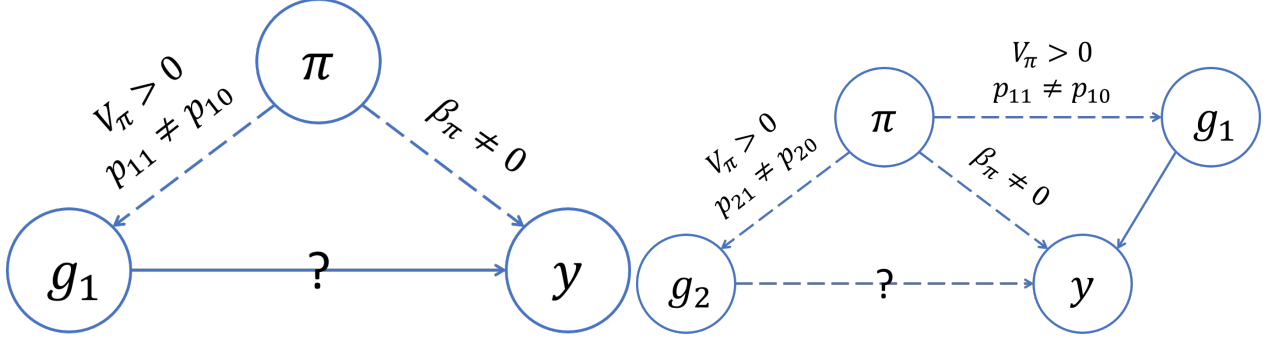


Figure 8: Conditions for confounding by global ancestry in GWAS.

(A) Global ancestry confounds the association at the causal variant (Variant 1) if there is ancestral heterogeneity in the population ($V_\pi > 0$), the causal variant has different allele frequencies in the ancestral populations ($p_{11} \neq p_{10}$), and global ancestry has a direct effect on the trait ($\beta_\pi \neq 0$).

(B) Global ancestry can confound the association at an unlinked neutral variant (Variant 2) even if global ancestry does not have a direct effect on the trait, provided that there is ancestral heterogeneity ($V_\pi > 0$) and both the causal variant and the variant being tested have different allele frequencies in the ancestral population ($p_{11} \neq p_{10}, p_{21} \neq p_{20}$).

model will yield a biased estimate of the effect size of the causal variant ($E[\hat{\beta}_1] \neq \beta_1$) unless there is no ancestral heterogeneity (i.e., $V_\pi = 0$), global ancestry does not have a direct effect on the trait (i.e., $\beta_\pi = 0$), or the causal variant does not have different allele frequencies in the ancestral populations (i.e., $p_{11} = p_{10}$). We see, also, that the model can yield a biased effect size at the unlinked neutral variant ($E[\hat{\beta}_2] \neq 0$) even if global ancestry does not have a direct effect on the trait, provided that both the causal variant and the variant being tested have allele frequencies that differ between the two ancestral populations (i.e., $p_{11} \neq p_{10}$ and $p_{21} \neq p_{20}$). These biased effect size estimates at neutral variants will translate into spurious associations as sample sizes increase, just as we saw in our simulations (Figure 6A and Supplemental Figure 14). These results are summarized in Figure 8 and underscore the importance of adjusting for ancestral heterogeneity even when global ancestry does not have a direct effect on the trait.

To emulate the idea of adjusting for principal components that adjust for local genomic features, we also consider a scenario in which our GWAS model adjusts for two “principal components”. We assume that the first principal component captures global ancestry (i.e.,

$\mathbf{u}_1 = \boldsymbol{\pi}$) but the second principal component captures some feature other than global ancestry (i.e., $\mathbf{u}_2 = \mathbf{z}$ for some variable z). Then, we can show that the expected effect size estimates at the causal variant and an unlinked neutral variant will be

$$E[\hat{\beta}_1] = \beta_1$$

$$E[\hat{\beta}_2] = 0 + \beta_1 \frac{-V_\pi E\{\text{Cov}(g_1, z | \boldsymbol{\pi})\} E\{\text{Cov}(g_2, z | \boldsymbol{\pi})\}}{V_z(V_\pi V_{g_2} - C_{g_2, \pi}^2) - V_\pi C_{g_2, z}^2 + C_{\pi, z}(2C_{g_2, \pi}C_{g_2, z} - V_{g_2}C_{\pi, z})},$$

where $V_a = \text{Var}(a)$ and $C_{a,b} = \text{Cov}(a, b)$. We see that this model adjusting for an extraneous principal component will yield an unbiased effect size estimate at the causal variant, but the same is not true for the unlinked neutral variant. In particular, the effect size estimate at this neutral variant will be biased away from zero when there is ancestral heterogeneity (i.e., $V_\pi \neq 0$) and the second principal component is correlated with both the causal variant and the variant being tested (i.e., $\text{Cov}(g_1, z | \boldsymbol{\pi}) \neq 0$ and $\text{Cov}(g_2, z | \boldsymbol{\pi}) \neq 0$). In other words, these results indicate that a model that adjusts for a PC that captures genotype at the causal variant as well as a second variant that is not associated with the trait, then spurious associations will arise at that second neutral variant in large enough samples. This is exactly what we observe in our simulations (Figure 6C, Figure 7D, Figure 7E). However, if the extra PC does not capture genotype at the causal variant, then spurious associations will not arise (Figure 6F, Figure 7C).

Proofs and simulations validating these analytic results are available in the Appendix.

4 Discussion

Need to address ancestral heterogeneity in admixed populations

- we observe considerable heterogeneity in global ancestry proportions in admixed populations studied here, as in other studies
- well-established that global ancestry is a potential confounding variable

- this confounding can exist even if global ancestry does not have a direct effect on the trait (as demonstrated by our simulation studies and theoretical results)
- → important to carefully measure and adjust for ancestral heterogeneity in GWAS in admixed populations

Comparing (naive) PCs and admixture proportions

- both widely used for measuring and adjusting for ancestral heterogeneity
- in AA, first PC correlated with global ancestry but later PCs are not (in HL: TBD)
- instead, later PCs often capture local genomic features (e.g., regions with extensive LD)
- while this has been documented before, note that, in contrast to what has been observed in EUR, we see that PCs seem to capture SNPs on more than one chromosome (multiple peaks in SNP loading plots); whereas in EUR we often just see one peak (cite Zou, Prive, other examples?) → why? LD patterns in admixed pops differ from those in EUR

[... for discussion:

- why is this happening? (LD)
- how does what we see compare to what's been observed in Europeans?
- does LD pruning universally fix the problem (i.e., does it seem to work better in some samples than others)? how many PCs does it help (i.e., what do PCs 5–10 look like)?
- why do we think exclusions didn't work? (high LD regions identified in Europeans, patterns of LD differ—more extensive—in admixed populations)

...]

Spurious associations

- adjusting for these PCs can lead to spurious associations
- this is due to a phenomenon known as collider bias
- ADD: what do theory and sims tell us about when/how likely a spurious association is to occur?
- ADD: could spurious associations replicate? (given that peaks often occur in similar places across datasets)

Impact of LD pruning and removing high LD regions

- after LD pruning, PCs no longer exhibit patterns of being driven by select few SNPs (at least for PCs 2-4)
- note that we had to use smaller r^2 and wider windows than often recommended in literature for this to be true → why? LD patterns in admixed pops differ from those in EUR
- excluding previously-identified high LD regions doesn't seem to be as effective → why? LD patterns in admixed pops differ from those in EUR
- note, too, that even strict LD pruning doesn't seem to remove all correlation between SNPs and genotypes (e.g., later PCs in WHI, TOPMed COPDGene)

Recommendations

- If using PCs, carefully inspect SNP loadings and/or correlation between PCs and genotypes
- If using PCs, don't use more than you need
- Consider using global ancestry proportions (although further work is needed to reliably capture sub-continental structure)

5 Appendix

- theoretical results
- proofs
- simulations validating theory

Supplemental Data

Supplemental Data include [... ?? ...] figures and [... ?? ...] tables.

Declaration of Interests

The authors declare no competing interests.

Acknowledgments

K.E.G. was supported by the National Science Foundation Graduate Research Fellowship Program under grant no. DGE-1256082. Any opinions, findings, and conclusions or recommendations expressed in this material are those of the author(s) and do not necessarily reflect the views of the National Science Foundation.

Web Resources

[GitHub Repository](#): lists of regions to exclude, code for LD pruning, excluding, and plotting loadings

Data and Code Availability

References

- [1] Parra, E. J., Marcini, A., Akey, J., Martinson, J., Batzer, M. A., Cooper, R., Forrester, T., Allison, D. B., Deka, R., Ferrell, R. E. *et al.* (1998). Estimating african american admixture proportions by use of population-specific alleles. *The American Journal of Human Genetics* *63*, 1839–1851.
- [2] Tishkoff, S. A., Reed, F. A., Friedlaender, F. R., Ehret, C., Ranciaro, A., Froment, A., Hirbo, J. B., Awomoyi, A. A., Bodo, J.-M., Doumbo, O. *et al.* (2009). The genetic structure and history of africans and african americans. *Science* *324*, 1035–1044.
- [3] Bryc, K., Auton, A., Nelson, M. R., Oksenberg, J. R., Hauser, S. L., Williams, S., Froment, A., Bodo, J.-M., Wambebe, C., Tishkoff, S. A. *et al.* (2010). Genome-wide patterns of population structure and admixture in west africans and african americans. *Proceedings of the National Academy of Sciences* *107*, 786–791.
- [4] Bryc, K., Velez, C., Karafet, T., Moreno-Estrada, A., Reynolds, A., Auton, A., Hammer, M., Bustamante, C. D., and Ostrer, H. (2010). Genome-wide patterns of population structure and admixture among hispanic/latino populations. *Proceedings of the National Academy of Sciences* *107*, 8954–8961.
- [5] Conomos, M. P., Laurie, C. A., Stilp, A. M., Gogarten, S. M., McHugh, C. P., Nelson, S. C., Sofer, T., Fernández-Rhodes, L., Justice, A. E., Graff, M. *et al.* (2016). Genetic diversity and association studies in us hispanic/latino populations: applications in the hispanic community health study/study of latinos. *The American Journal of Human Genetics* *98*, 165–184.
- [6] Devlin, B. and Roeder, K. (1999). Genomic control for association studies. *Biometrics* *55*, 997–1004.

- [7] Price, A. L., Patterson, N. J., Plenge, R. M., Weinblatt, M. E., Shadick, N. A., and Reich, D. (2006). Principal components analysis corrects for stratification in genome-wide association studies. *Nature genetics* *38*, 904–909.
- [8] Marchini, J., Cardon, L. R., Phillips, M. S., and Donnelly, P. (2004). The effects of human population structure on large genetic association studies. *Nature Genetics* *36*, 512–517.
- [9] Price, A. L., Zaitlen, N. A., Reich, D., and Patterson, N. (2010). New approaches to population stratification in genome-wide association studies. *Nature Reviews Genetics* *11*, 459–463.
- [10] Need, A. C. and Goldstein, D. B. (2009). Next generation disparities in human genomics: concerns and remedies. *Trends in Genetics* *25*, 489–494.
- [11] Bustamante, C. D., Francisco, M., and Burchard, E. G. (2011). Genomics for the world. *Nature* *475*, 163–165.
- [12] Popejoy, A. B. and Fullerton, S. M. (2016). Genomics is failing on diversity. *Nature News* *538*, 161.
- [13] Hindorff, L. A., Bonham, V. L., Brody, L. C., Ginoza, M. E., Hutter, C. M., Manolio, T. A., and Green, E. D. (2018). Prioritizing diversity in human genomics research. *Nature Reviews Genetics* *19*, 175.
- [14] Manolio, T. A. (2019). Using the data we have: improving diversity in genomic research. *The American Journal of Human Genetics* *105*, 233–236.
- [15] Lander, E. S. and Schork, N. J. (1994). Genetic dissection of complex traits. *Science* *265*, 2037–2048.
- [16] Spielman, R. S., McGinnis, R. E., and Ewens, W. J. (1993). Transmission test for

- linkage disequilibrium: the insulin gene region and insulin-dependent diabetes mellitus (iddm). *American journal of human genetics* *52*, 506.
- [17] Yu, J., Pressoir, G., Briggs, W. H., Bi, I. V., Yamasaki, M., Doebley, J. F., McMullen, M. D., Gaut, B. S., Nielsen, D. M., Holland, J. B. *et al.* (2006). A unified mixed-model method for association mapping that accounts for multiple levels of relatedness. *Nature Genetics* *38*, 203–208.
- [18] Kang, H. M., Sul, J. H., Service, S. K., Zaitlen, N. A., Kong, S.-y., Freimer, N. B., Sabatti, C., Eskin, E. *et al.* (2010). Variance component model to account for sample structure in genome-wide association studies. *Nature Genetics* *42*, 348–354.
- [19] Yang, J., Zaitlen, N. A., Goddard, M. E., Visscher, P. M., and Price, A. L. (2014). Advantages and pitfalls in the application of mixed-model association methods. *Nature Genetics* *46*, 100–106.
- [20] Pritchard, J. K., Stephens, M., Rosenberg, N. A., and Donnelly, P. (2000). Association mapping in structured populations. *The American Journal of Human Genetics* *67*, 170–181.
- [21] Tang, H., Peng, J., Wang, P., and Risch, N. J. (2005). Estimation of individual admixture: analytical and study design considerations. *Genetic Epidemiology* *28*, 289–301.
- [22] Falush, D., Stephens, M., and Pritchard, J. K. (2003). Inference of population structure using multilocus genotype data: linked loci and correlated allele frequencies. *Genetics* *164*, 1567–1587.
- [23] Alexander, D. H., Novembre, J., and Lange, K. (2009). Fast model-based estimation of ancestry in unrelated individuals. *Genome Research* *19*, 1655–1664.
- [24] Maples, B. K., Gravel, S., Kenny, E. E., and Bustamante, C. D. (2013). Rfmix: a

- discriminative modeling approach for rapid and robust local-ancestry inference. *The American Journal of Human Genetics* *93*, 278–288.
- [25] Zheng, X., Levine, D., Shen, J., Gogarten, S. M., Laurie, C., and Weir, B. S. (2012). A high-performance computing toolset for relatedness and principal component analysis of snp data. *Bioinformatics* *28*, 3326–3328.
- [26] Conomos, M. P., Miller, M. B., and Thornton, T. A. (2015). Robust inference of population structure for ancestry prediction and correction of stratification in the presence of relatedness. *Genetic epidemiology* *39*, 276–293.
- [27] Novembre, J., Johnson, T., Bryc, K., Kutalik, Z., Boyko, A. R., Auton, A., Indap, A., King, K. S., Bergmann, S., Nelson, M. R. *et al.* (2008). Genes mirror geography within europe. *Nature* *456*, 98–101.
- [28] Patterson, N., Price, A. L., and Reich, D. (2006). Population structure and eigenanalysis. *PLoS Genet* *2*, e190.
- [29] McVean, G. (2009). A genealogical interpretation of principal components analysis. *PLoS Genet* *5*, e1000686.
- [30] Reed, E., Nunez, S., Kulp, D., Qian, J., Reilly, M. P., and Foulkes, A. S. (2015). A guide to genome-wide association analysis and post-analytic interrogation. *Statistics in Medicine* *34*, 3769–3792.
- [31] Raska, P., Iversen, E., Chen, A., Chen, Z., Fridley, B. L., Permuth-Wey, J., Tsai, Y.-Y., Vierkant, R. A., Goode, E. L., Risch, H. *et al.* (2012). European american stratification in ovarian cancer case control data: the utility of genome-wide data for inferring ancestry. *Plos one* *7*, e35235.
- [32] Reiner, A. P., Beleza, S., Franceschini, N., Auer, P. L., Robinson, J. G., Kooperberg, C., Peters, U., and Tang, H. (2012). Genome-wide association and population genetic

- analysis of c-reactive protein in african american and hispanic american women. *The American Journal of Human Genetics* *91*, 502–512.
- [33] Daya, M., Rafaels, N., Brunetti, T. M., Chavan, S., Levin, A. M., Shetty, A., Gignoux, C. R., Boorgula, M. P., Wojcik, G., Campbell, M. *et al.* (2019). Association study in african-admixed populations across the americas recapitulates asthma risk loci in non-african populations. *Nature Communications* *10*, 1–13.
- [34] Abegaz, F., Chaichoompu, K., Génin, E., Fardo, D. W., König, I. R., Mahachie John, J. M., and Van Steen, K. (2019). Principals about principal components in statistical genetics. *Briefings in Bioinformatics* *20*, 2200–2216.
- [35] Mathieson, I. and McVean, G. (2012). Differential confounding of rare and common variants in spatially structured populations. *Nature Genetics* *44*, 243–246.
- [36] Liu, N., Zhao, H., Patki, A., Limdi, N. A., and Allison, D. B. (2011). Controlling population structure in human genetic association studies with samples of unrelated individuals. *Statistics and its interface* *4*, 317.
- [37] Abdellaoui, A., Hottenga, J.-J., De Knijff, P., Nivard, M. G., Xiao, X., Scheet, P., Brooks, A., Ehli, E. A., Hu, Y., Davies, G. E. *et al.* (2013). Population structure, migration, and diversifying selection in the netherlands. *European Journal of Human Genetics* *21*, 1277–1285.
- [38] Weale, M. E. (2010). Quality control for genome-wide association studies. *Genetic Variation* , 341–372.
- [39] Consortium, W. T. C. C. *et al.* (2007). Genome-wide association study of 14,000 cases of seven common diseases and 3,000 shared controls. *Nature* *447*, 661.
- [40] Tian, C., Plenge, R. M., Ransom, M., Lee, A., Villoslada, P., Selmi, C., Klareskog,

- L., Pulver, A. E., Qi, L., Gregersen, P. K. *et al.* (2008). Analysis and application of european genetic substructure using 300 k snp information. *PLoS Genet* *4*, e4.
- [41] Price, A. L., Weale, M. E., Patterson, N., Myers, S. R., Need, A. C., Shianna, K. V., Ge, D., Rotter, J. I., Torres, E., Taylor, K. D. *et al.* (2008). Long-range ld can confound genome scans in admixed populations. *The American Journal of Human Genetics* *83*, 132–135.
- [42] Zou, F., Lee, S., Knowles, M. R., and Wright, F. A. (2010). Quantification of population structure using correlated snps by shrinkage principal components. *Human Heredity* *70*, 9–22.
- [43] Laurie, C. C., Doheny, K. F., Mirel, D. B., Pugh, E. W., Bierut, L. J., Bhangale, T., Boehm, F., Caporaso, N. E., Cornelis, M. C., Edenberg, H. J. *et al.* (2010). Quality control and quality assurance in genotypic data for genome-wide association studies. *Genetic Epidemiology* *34*, 591–602.
- [44] Privé, F., Luu, K., Blum, M. G., McGrath, J. J., and Vilhjálmsdóttir, B. J. (2020). Efficient toolkit implementing best practices for principal component analysis of population genetic data. *Bioinformatics* *36*, 4449–4457.
- [45] Purcell, S., Neale, B., Todd-Brown, K., Thomas, L., Ferreira, M. A., Bender, D., Maller, J., Sklar, P., De Bakker, P. I., Daly, M. J. *et al.* (2007). Plink: a tool set for whole-genome association and population-based linkage analyses. *The American Journal of Human Genetics* *81*, 559–575.
- [46] Fellay, J., Shianna, K. V., Ge, D., Colombo, S., Ledergerber, B., Weale, M., Zhang, K., Gumb, C., Castagna, A., Cossarizza, A. *et al.* (2007). A whole-genome association study of major determinants for host control of hiv-1. *Science* *317*, 944–947.
- [47] Yu, K., Wang, Z., Li, Q., Wacholder, S., Hunter, D. J., Hoover, R. N., Chanock, S.,

- and Thomas, G. (2008). Population substructure and control selection in genome-wide association studies. *PLoS one* *3*, e2551.
- [48] Nelson, M. R., Bryc, K., King, K. S., Indap, A., Boyko, A. R., Novembre, J., Briley, L. P., Maruyama, Y., Waterworth, D. M., Waeber, G. *et al.* (2008). The population reference sample, popres: a resource for population, disease, and pharmacological genetics research. *The American Journal of Human Genetics* *83*, 347–358.
- [49] Anderson, C. A., Pettersson, F. H., Clarke, G. M., Cardon, L. R., Morris, A. P., and Zondervan, K. T. (2010). Data quality control in genetic case-control association studies. *Nature Protocols* *5*, 1564–1573.
- [50] Zhang, Y., Guan, W., and Pan, W. (2013). Adjustment for population stratification via principal components in association analysis of rare variants. *Genetic epidemiology* *37*, 99–109.
- [51] Galinsky, K. J., Bhatia, G., Loh, P.-R., Georgiev, S., Mukherjee, S., Patterson, N. J., and Price, A. L. (2016). Fast principal-component analysis reveals convergent evolution of adh1b in europe and east asia. *The American Journal of Human Genetics* *98*, 456–472.
- [52] Privé, F., Aschard, H., Ziyatdinov, A., and Blum, M. G. (2018). Efficient analysis of large-scale genome-wide data with two r packages: bigstatsr and bigsnpr. *Bioinformatics* *34*, 2781–2787.
- [53] Hays, J., Hunt, J. R., Hubbell, F. A., Anderson, G. L., Limacher, M., Allen, C., and Rossouw, J. E. (2003). The Women’s Health Initiative recruitment methods and results. *Annals of Epidemiology* *13*, S18–S77.
- [54] Conomos, M. P., Reiner, A. P., Weir, B. S., and Thornton, T. A. (2016). Model-free estimation of recent genetic relatedness. *The American Journal of Human Genetics* *98*, 127–148.

- [55] Jun, G., Wing, M. K., Abecasis, G. R., and Kang, H. M. (2015). An efficient and scalable analysis framework for variant extraction and refinement from population-scale dna sequence data. *Genome Research* *25*, 918–925.
- [56] Taliun, D., Harris, D. N., Kessler, M. D., Carlson, J., Szpiech, Z. A., Torres, R., Taliun, S. A. G., Corvelo, A., Gogarten, S. M., Kang, H. M. *et al.* (2021). Sequencing of 53,831 diverse genomes from the nhlbi topmed program. *Nature* *590*, 290–299.
- [57] Danecek, P., Bonfield, J. K., Liddle, J., Marshall, J., Ohan, V., Pollard, M. O., Whitwham, A., Keane, T., McCarthy, S. A., Davies, R. M. *et al.* (2021). Twelve years of samtools and bcftools. *Gigascience* *10*, giab008.
- [58] Consortium, I. H. . *et al.* (2010). Integrating common and rare genetic variation in diverse human populations. *Nature* *467*, 52.
- [59] Grinde, K. E., Brown, L. A., Reiner, A. P., Thornton, T. A., and Browning, S. R. (2019). Genome-wide significance thresholds for admixture mapping studies. *The American Journal of Human Genetics* *104*, 454–465.
- [60] Parker, M. M., Foreman, M. G., Abel, H. J., Mathias, R. A., Hetmanski, J. B., Crapo, J. D., Silverman, E. K., Beaty, T. H., and Investigators, C. (2014). Admixture mapping identifies a quantitative trait locus associated with fev1/fvc in the copdgene study. *Genetic Epidemiology* *38*, 652–659.
- [61] Kirk, J. L. (2016). *Statistical methods for inferring population structure with human genome sequence data*. PhD thesis, University of Washington.
- [62] Pe'er, I., Yelensky, R., Altshuler, D., and Daly, M. J. (2008). Estimation of the multiple testing burden for genomewide association studies of nearly all common variants. *Genetic Epidemiology* *32*, 381–385.

- [63] Jannet, A.-S., Ehret, G., and Perneger, T. (2015). $P \leq 5 \times 10^{-8}$ has emerged as a standard of statistical significance for genome-wide association studies. *Journal of Clinical Epidemiology* *68*, 460–465.
- [64] Carty, C. L., Johnson, N. A., Hutter, C. M., Reiner, A. P., Peters, U., Tang, H., and Kooperberg, C. (2012). Genome-wide association study of body height in African Americans: The Women’s Health Initiative SNP Health Association Resource (SHARe). *Human Molecular Genetics* *21*, 711–720.

Figure Titles and Legends

Tables

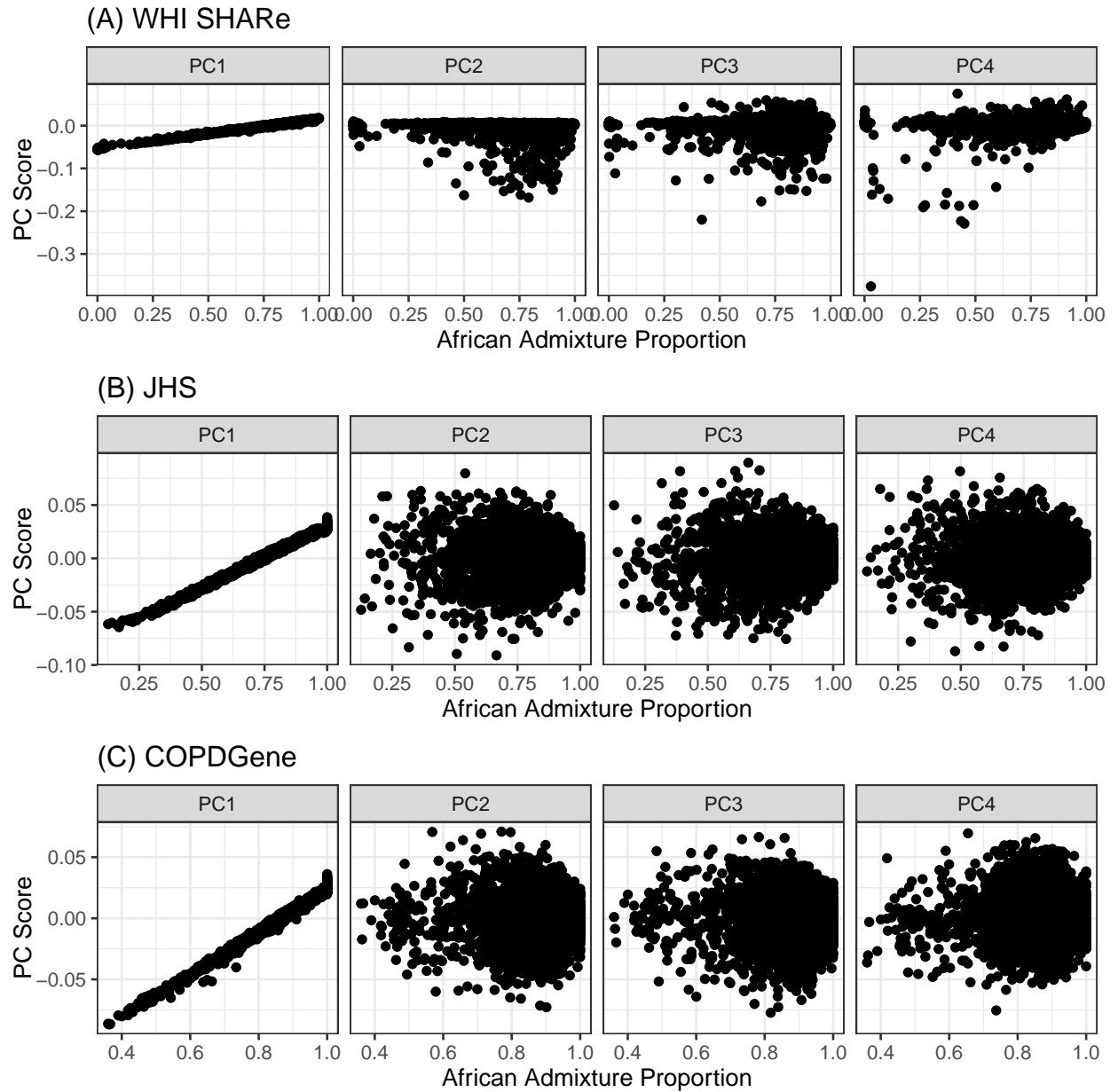


Figure 9: Scatterplots of estimated African admixture proportions versus the first four PCs in WHI SHARe (Panel A), TOPMed JHS (Panel B), and TOPMed COPDGene (Panel C) African Americans. Here we consider PCs that were generated after LD pruning ($r^2 = 0.1$, window size = 0.5 Mb) and filtering previously identified high-LD regions (1).

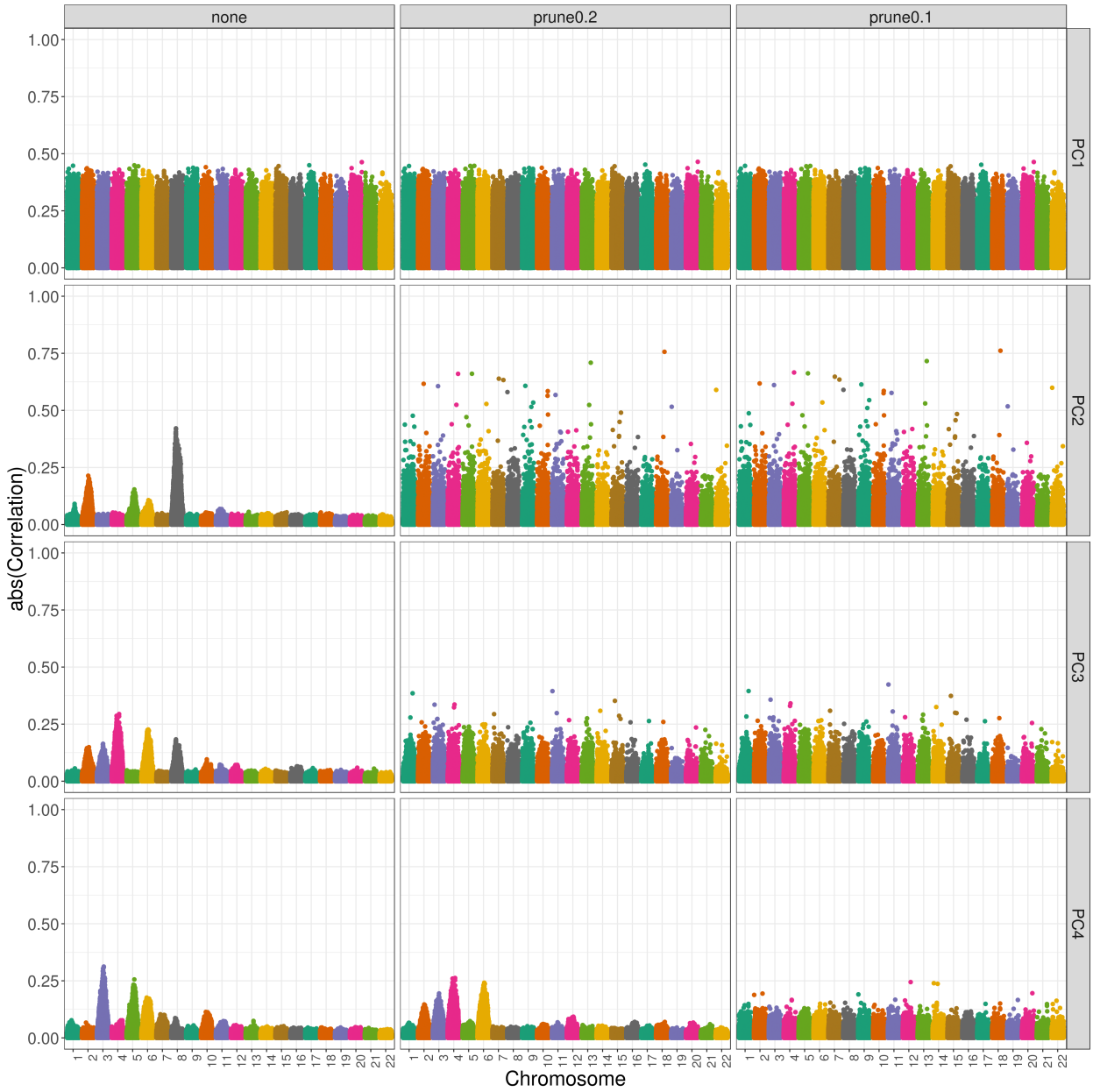


Figure 10: Correlation between PCs and genotypes in WHI SHARe African Americans using different LD pruning thresholds. Each panel plots the absolute value of the correlation between principal components and genotypes (on the y-axis) versus the position along the genome (x-axis). Panels are organized vertically according to which PC is being investigated (1, 2, 3, 4) and horizontally according to what r^2 threshold was used when running LD pruning prior to PCA (*none*: no LD pruning, *prune0.2*: LD pruning with an r^2 threshold of 0.2 and window size of 0.5 Mb, and *prune0.1*: LD pruning with an r^2 threshold of 0.1 and window size of 0.5 Mb).

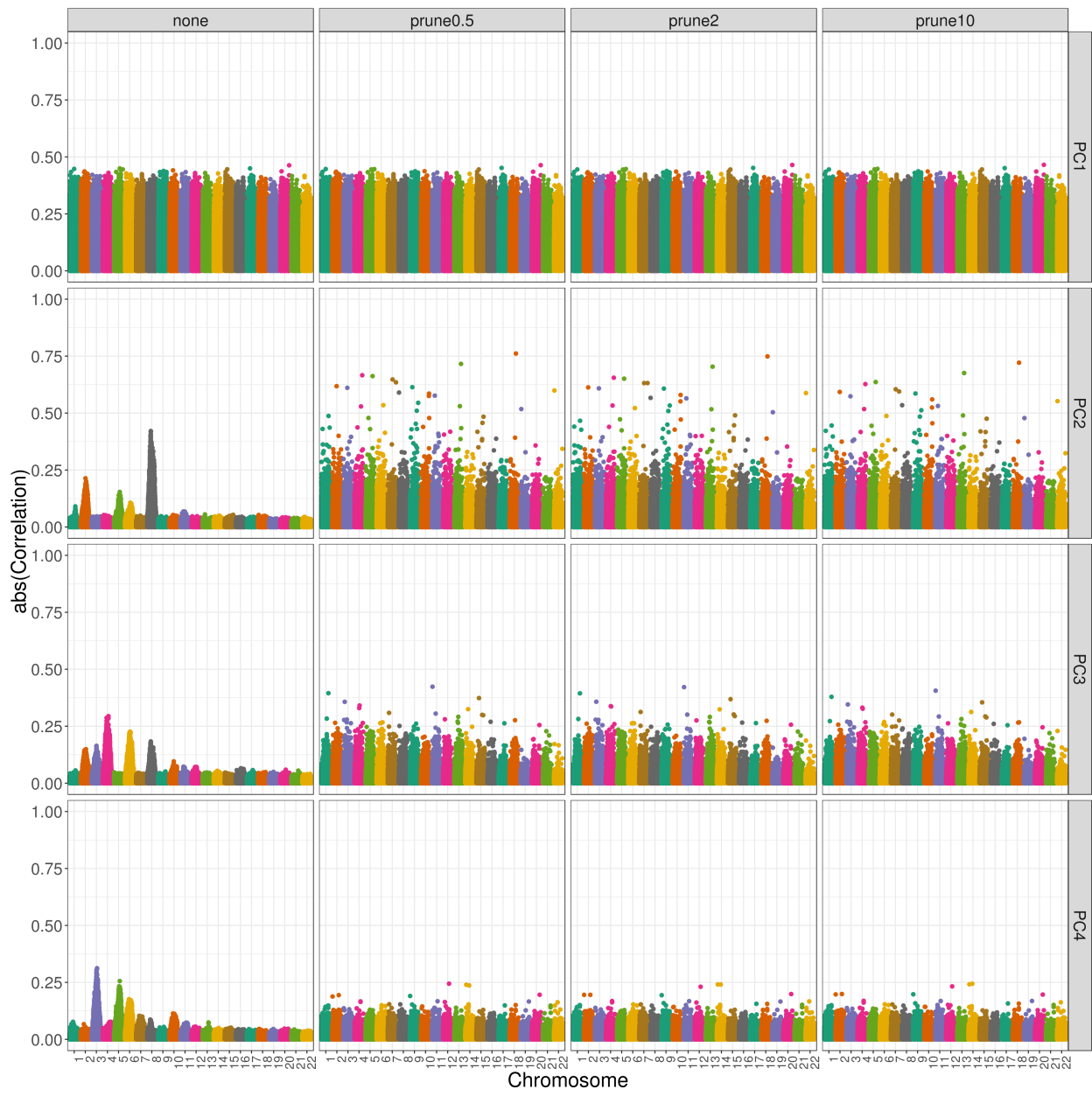


Figure 11: Correlation between PCs and genotypes in WHI SHARe African Americans using different LD pruning window sizes. Each panel plots the absolute value of the correlation between principal components and genotypes (on the y-axis) versus the position along the genome (x-axis). Panels are organized vertically according to which PC is being investigated (1, 2, 3, 4) and horizontally according to what window size was used when running LD pruning prior to PCA (*none*: no LD pruning, *prune0.5*: LD pruning with an r^2 threshold of 0.1 and window size of 0.5 Mb, *prune2*: LD pruning with an r^2 threshold of 0.1 and window size of 2 Mb, and *prune10*: LD pruning with an r^2 threshold of 0.1 and window size of 10 Mb).

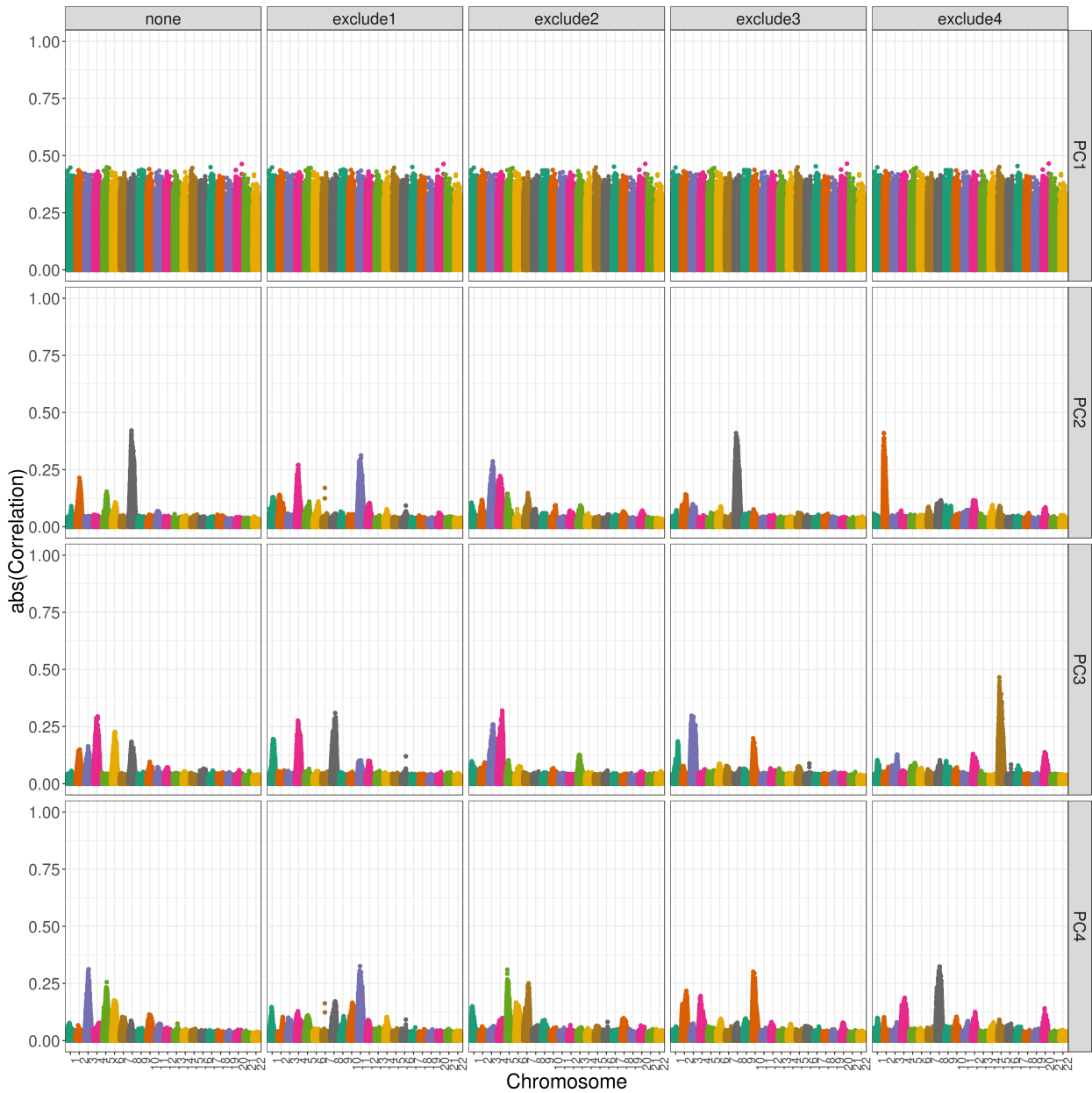


Figure 12: Correlation between PCs and genotypes in WHI SHARe African Americans after multiple rounds of data-based exclusions. Each panel plots the absolute value of the correlation between principal components and genotypes (on the y-axis) versus the position along the genome (x-axis). Panels are organized vertically according to which PC is being investigated (1, 2, 3, 4) and horizontally according to the number of iterations of our procedure for excluding regions highly correlated with PCs that were implemented prior to PCA (*none*: no exclusions, *exclude1*: one round of exclusions, *exclude2*: two rounds of exclusions, etc.).

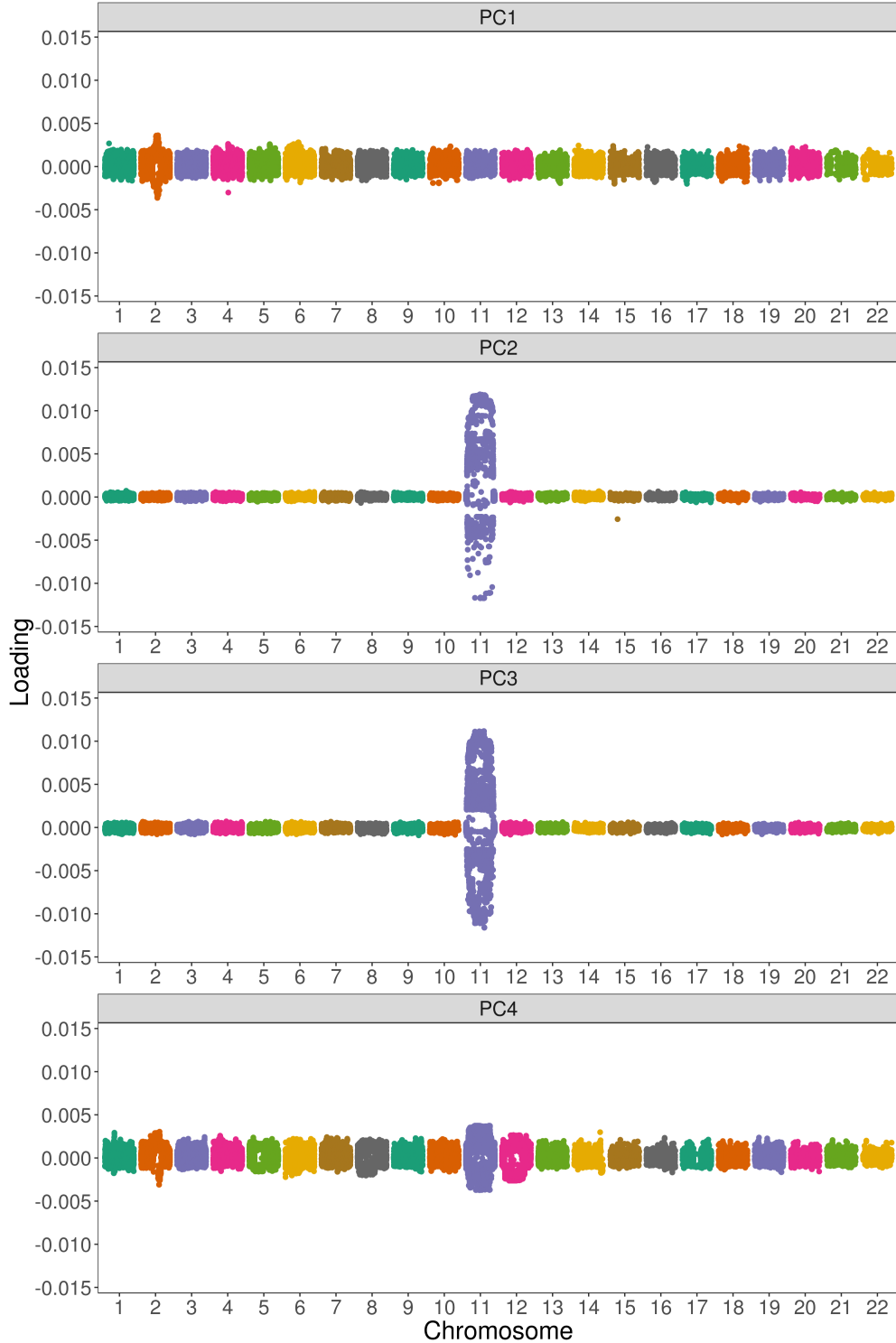


Figure 13: SNP loadings for naively generated PCs in COPDGene European Americans. Each panel plots the principal component loading (y-axis) versus the position along the genome (x-axis) for each variant. Panels are organized vertically according to which PC is being investigated (1, 2, 3, 4). Unlike in admixed populations, we see a single peak on chromosome 11.

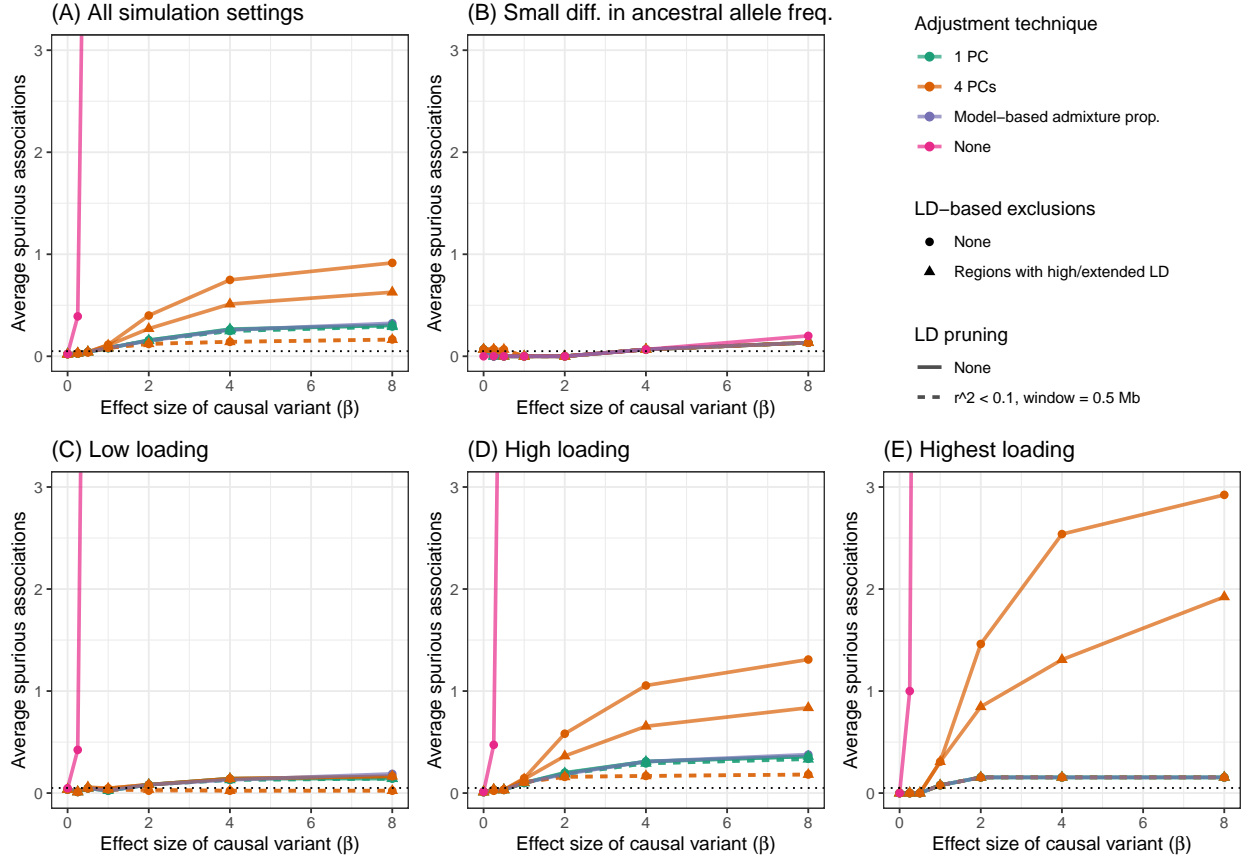


Figure 14: Comparison of the number of spurious associations in genome-wide association studies in WHI SHARe African Americans using different approaches to adjust for ancestral heterogeneity. Panels display the average number of spurious associations that were observed across (A) all simulation settings, or across the subset of simulation settings in which the causal variant has (B) a small difference in ancestral allele frequencies, (C) low SNP loadings for each of the first four PCs, (D) a high SNP loading for at least one of the first four PCs, or (E) the highest SNP loading on its chromosome for one of the first four PCs. Within each panel, we compare the number of spurious associations when GWAS models adjust for model-based admixture proportions, 1 PC (with or without LD pruning and/or Table 1 exclusions), or 4 PCs (with or without LD pruning and/or Table 1 exclusions). Results shown here are for simulated traits with a single causal variant, with effect size (β) ranging from 0 to 8.